Numerical Simulations to Investigate the Efficiency of Joint Designs for the Electro-Magnetic Welding (EMW) of the Ring-shaft Assembly

H. Kim [1], J. Gould [1], J. Shang [2], A. Yadav [3], R. Meyer [3], Pierre L'Eplattenier [4]

[1]*Edison Welding Institute, 1250 Arthur E. Adams Drive, Columbus, Ohio 43221-3585, U.S.*
[2]*American Trim, 999 West Ground Ave., Lima, Ohio 45801, U.S.*
[3]*Caterpillar Inc., Peoria, Illinois 61656-1875, U.S.*
[4]*Livermore Software Technology Corporation, 7374 Las Positas Road, Livermore, CA 94551*

Abstract

In this study, numerical simulations on electro-magnetic welding (EMW) were conducted for dissimilar materials joint of the ring-shaft assembly. LS-DYNA® electromagnetism module was adopted to simulate the EMW process. Simulation results were correlated with the EMW experimental works with two different joint designs, single and double flared lap joint. Two different materials, aluminum 6061-T4 and copper, C40, were used for the driver ring material on the stationary steel shaft. LS-DYNA simulation model was used to investigate the effects of impact angle and velocity on surface-layer bonding and joining efficiency of the driver ring on a steel shaft. Analytical modeling was also conducted to estimate the magnetic pressure between the coil and the ring. Experimentally, a 90-KJ machine was used at different energy levels. From these experiments, the double flared lap joint showed better joint efficiency and the copper showed better adhesion than aluminum at same energy levels. The performance of joint was evaluated by push-off testing. A double flared copper ring at 45-KJ gave the best performance of joint, and exceeded the required axial thrust load requirement. From the metallographic analysis, the interface of joint did not show the metallurgical bonding, however, strong mechanical interlocking was achieved. This study demonstrates the viability of EMW process for dissimilar material joining.

KEYWORDS
Electro-magnetic welding (EMW), Dissimilar materials joining

INTRODUCTION

Electro-magnetic welding (EMW) is a high-speed process used for joining tubular structures. EMW is applicable to a nominally lap-type joint of tube-to-tube or tube-to-bar configurations. EMW uses the magnetic repulsion between two opposing magnetic fields to drive a conductive metal. The energy stored in a capacitor bank is discharged usually within 20 ms, through an induction coil that encompasses the parts to be joined. The magnetic field produced by the coil crosses the workpiece, generating eddy currents in the workpiece. This current produces its own magnetic field. These two opposing magnetic fields at the coil and workpiece induce a repulsion force between the coil and the workpiece. The theory behind this repulsion is well explained by Lenz's law. This repulsion causes the outer workpiece to drive and impact the inner workpiece at very high velocity (Figure 1). These

impact velocities, combined with an appropriate impact angle, are sufficient to create localized deformation and subsequent bonding.

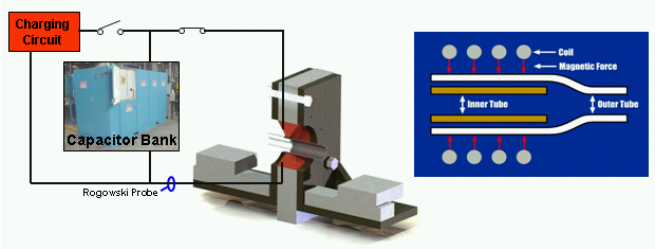

Figure 1. EMW System (Left) and the Configuration of Coil/Workpieces (Right)

The resulting bond occurs with a morphology quite similar to that of explosion bonding. The process has shown particular promise for dissimilar materials joining that is usually hard to obtain by arc welding. Given the short cycle times, as well as the capability to join dissimilar material combinations, the process has attracted considerable attention in a range of industrial applications the aerospace, automotive, and electronics industries.

OBJECTIVE

The objective of this study is to reliably predict the effects of impact angle and velocity on surface-layer bonding and joining efficiency of the driver ring on a steel shaft. Figure 2 shows the required assembly design. A ring has to be welded on the steel shaft and this ring played as a mechanical stopper in actual service condition. Conventionally, this joint was made by arc welding. However, the joint strength is required to meet to a minimum 20-KN axial thrust load in service condition.

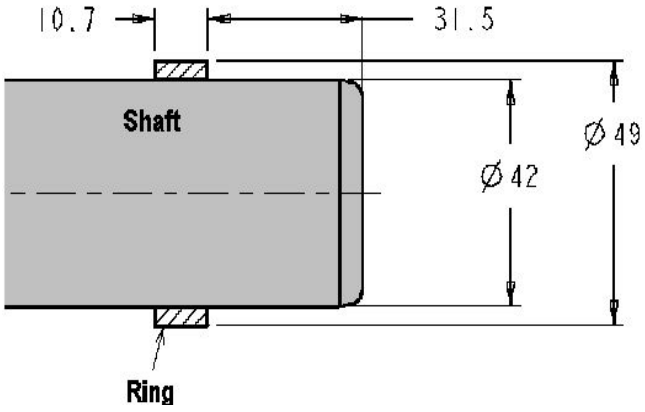

Figure 2. The Ring-Shaft Assembly (all units are in mm)

DESIGNS FOR WELD JOINT AND TOOLING

Baseline components and process requirements for EMW were designed to join the ring-shaft assembly. Two different designs (single- and double-flared rings and associated concentrator) were conceived to accelerate the ring during EMW process, as show in Figures 3 and 4, respectively. Single-flared ring was designed to have almost zero gap in radius between the steel bar and the ring. Double-flared ring was designed to have a 2-mm gap on radius. Increasing the gap can increase the impact speed of ring during EMW, but it is not appropriate for the single-flared ring, because it can cause unnecessary plastic deformation of 3-mm straight section (Figure 3) and this can result in the loss of discharging energy.

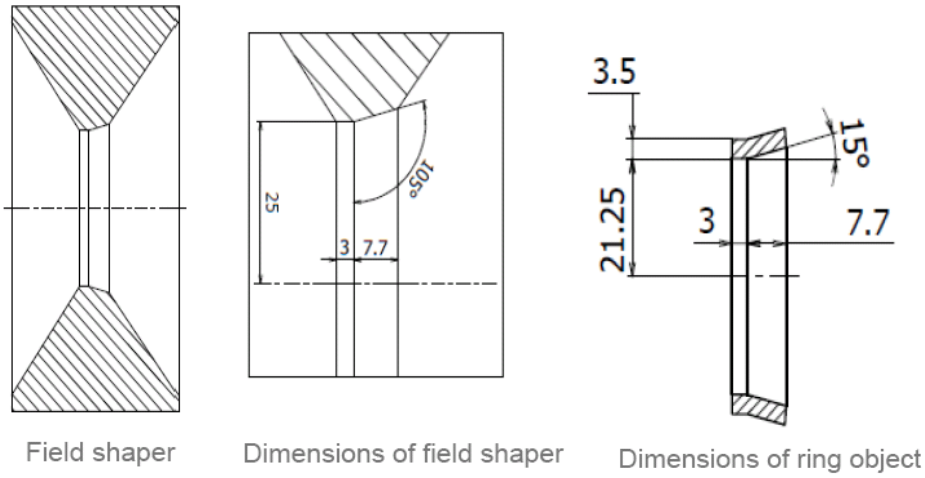

Figure 3. Schematic of Designs of Field Shaper and Ring Object (all units are mm)

The inclined angle of flared section of ring, namely *attack angle*, was recommended to be 15 degrees from extensive experimental work of EMW [Kojima et al., 1989 and Masumoto et al., 1985].

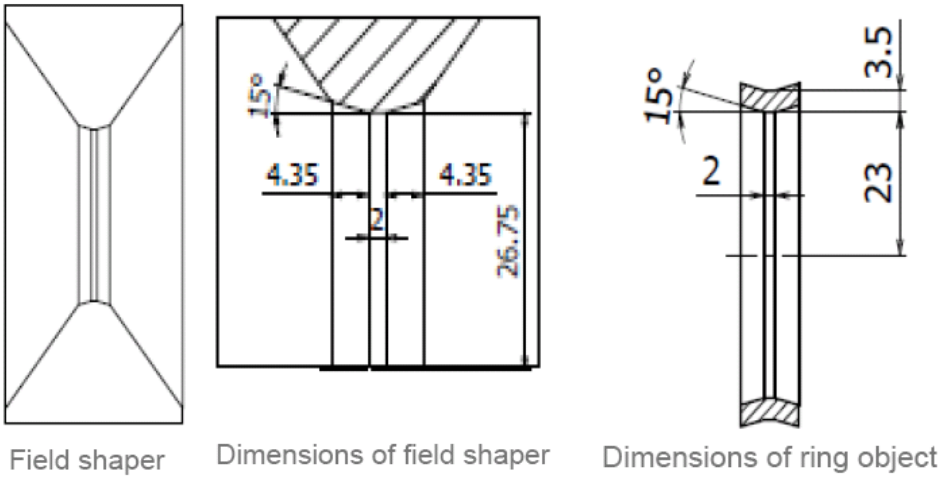

Figure 4. Schematic of Designs of Field Shaper and Double-Flared Ring Object (all units are mm)

Two different materials, aluminum (Al 6061-T4) and chromium copper alloy (C18200) were used for ring. Al 6061-T6 tubes with 49.5-mm outer diameter and 3.5-mm-thick were machined to 10.7-mm long, and then heat treated to Al 6061-T4 condition. After heat treatment, the rings were flared to have 15-degree attack angle with a forming die in the hydraulic press. Copper rings were heat treated at 650ºC for 1½ hour and quenched to water. The yield strength and tensile strength of Al 6061-T4 are 45 and 241-MPa, respectively. The yield strength and tensile strength of C18200 are 352-MPa and 365-MPa. The bars and rings were polished with sand papers, and then cleaned with acetone.

The double-flared samples were directly machined, because of difficulties in forming flares. Figure 5 showed both single- and double-flared samples. Figure 6 shows the initial position of double-flared ring into the halves of copper concentrator.

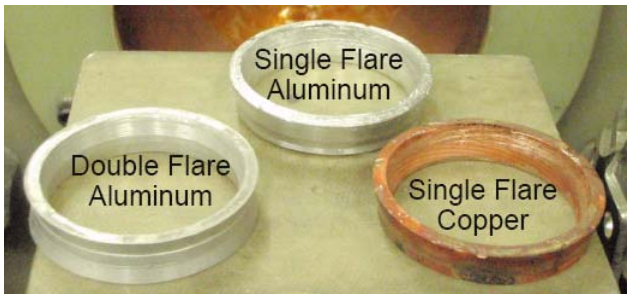

Figure 5. Single- and Double-Flared Aluminum and Copper Samples

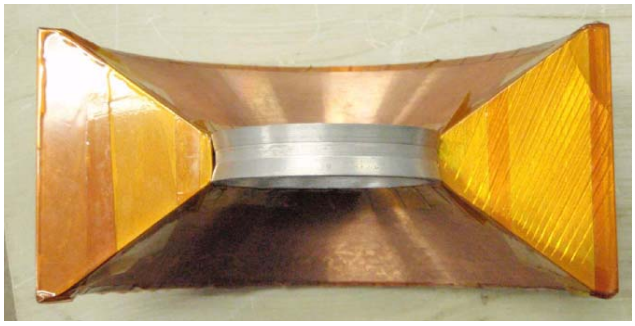

Figure 6. Double-Flared Ring and the Split Halve of Copper Concentrator

EXPERIMENTAL WORK

The welding experiments were conducted in a MAGNEFORM 90-KJ magnetic pulse welder. The machine is equipped with 30 capacitors, and each capacitor has capacitance of 60-μF. The charging voltage over the capacitor bank is up to 10-kV. The main coil, a copper concentrator, and fixture are shown in Figure 7. The split halves of the concentrator are assembled around the ring. This sub-assembly is inserted into the bore of the filed shaper. All pieces in the assembly are insulated from each other with the use of Kapton tape. The completed assembly is then inserted into the bore of the single turn coil.

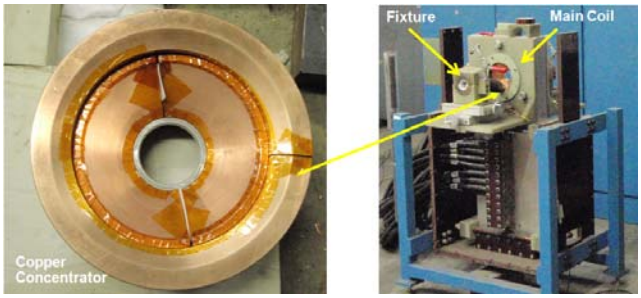

Figure 7. The Split Halves of the Copper Concentrator (Left) and EMW Experimental Setup (Right)

Welding trials were conducted in an iterative manner and the detailed test conditions are given in Table 1. The welded samples were selectively inspected by cutting the ring and checking if the ring was easily separated from steel bar. Push-off test and metallography were used to evaluate weld quality.

The push-off test was conducted by using the 66.7-kN Instron Machine with the ram speed of 19.05-mm/min. To hold the welded part during the testing, the annual fixture was used to fix a steel bar during the test. The maximum load and the displacement at the maximum load were measured from the machine.

Table 1. Testing Conditions.

Ring Material	Joint Design	Voltage (KV)	Energy (KJ)
Al 6061-T4	Single flared	4.47/5.20/6.32/ 7.75/8.94/9.49	18/24/30/36/ 72/81
	Double flared		
C18200	Single flared	5.20/6.32/7.07/ 7.75	24/36/45/54
	Double flared		

EXPERIMENTAL RESULTS

In EMW tests, most of the single-flared ring samples showed relatively weak joint with steel bar compared to the double-flared ring samples. Aluminum ring samples showed local melted edge as the discharge energy was increased, while the chromium copper alloy ring did not show any local melting at same or even higher levels of energy. Figure 8 shows double-flared aluminum samples tested at 24-KJ and 30-KJ. Figure 9 shows the double-flared copper sample tested at 45-KJ.

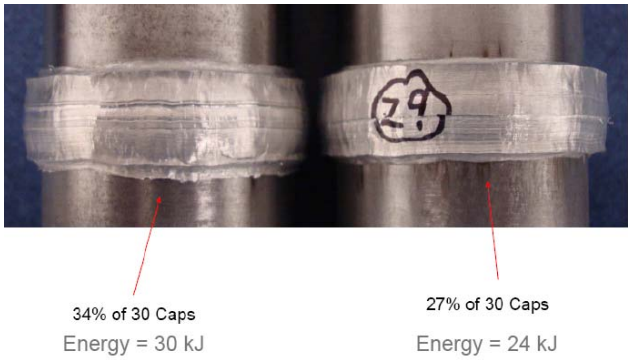

Figure 8. Aluminum Ring Samples Joined to Steel Bars

Figure 9. Copper Ring Sample Joined to Steel Bars at 45-KJ

Push-off test results are summarized in Table 2. Double-flared copper samples No.35 and No.37 tested at 45-KJ showed the maximum load to be about 80-kN and 62-kN, respectively.

Table 2. Push-Off Testing Results.

Sample ID	Ring material and design	Energy used for MPW	Maximum Load
		(kJ)	(kN)
9	Al dual flare with zero gap	54	16.87
10	Al single flare ring	54	17.05
11	Cu single flare ring	54	25.50
13	Al single flare ring	24	7.81
14	Cu single flare ring	24	4.18
24	Al dual flare with 2mm gap	24.3	40.08
27	Al dual flare with 2mm gap	36	19.55
30	Al dual flare with 2mm gap	30.6	32.05
33	Al dual flare with 2mm gap	24.3	24.88
34	Cu dual flare with 2mm gap	36	24.62
35	Cu dual flare with 2mm gap	45	79.79
37	Cu dual flare with 2mm gap	45	62.49

Micrographs at the joint interface were taken to inspect the weld line. However, there are no clear metallurgical bonding observed between steel and aluminum that are marked as CS and Al in Figure 10.

The copper ring sample also did not show any metallurgical bonding and after cutting the ring samples from joint, it was easily separated from steel bar. With these micrographic results, most of the joints were made by mechanical fitting without metallurgical bonding. Interestingly, this mechanical fitting showed significantly higher joint strength in push-off tests.

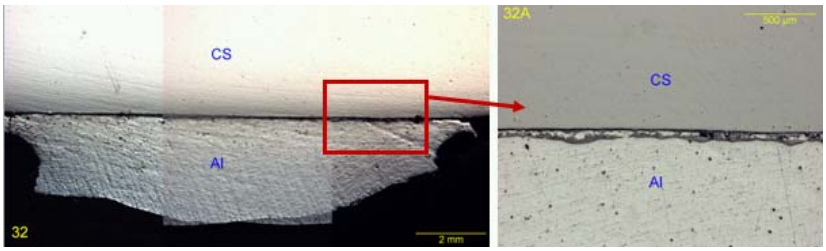

Figure 10. Micrographs of EMW Joint Area

ANALYTICAL RESULTS

Magnetic pulse pressure, P_m, was calculated by using the analytical equation (1) [Gourdin 1989 and Daehn 2005].

$$P_m = \frac{\mu_0 \cdot n^2 \cdot f_2}{2 \cdot l_s^{\,2}} \cdot I^2(t) \tag{1}$$

Where μ_0 = magnetic permeability , n = the number of coil turn, l_s=coil length,
f_2=the coupling factor between the primary and the secondary currents.

This analytical model does not consider any efficiency loss of current while it transfers from the main coil-to-copper concentrator and ring. The measured time-current curves were used to calculate the magnetic pulse pressures. Figure 11 and Figure 12 show the measured curves for the aluminum ring sample at 30.6-KJ and the copper ring sample at 45-KJ. The maximum magnetic pressure was calculated as 2.39-GPa for the aluminum ring sample and 4.05-GPa for the copper ring sample.

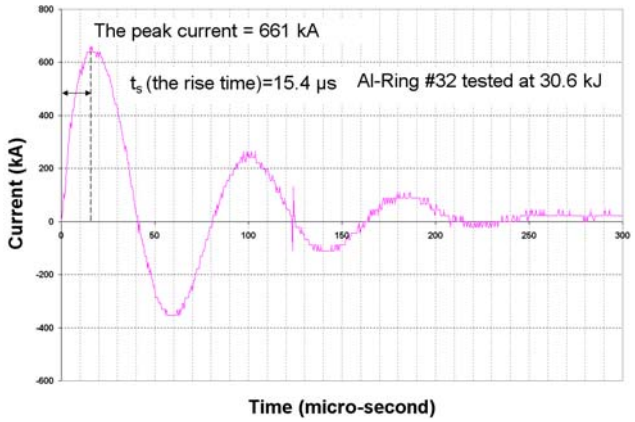

Figure 11. Measured Time-Current Profile for Aluminum Ring Tested at 30.6-KJ.

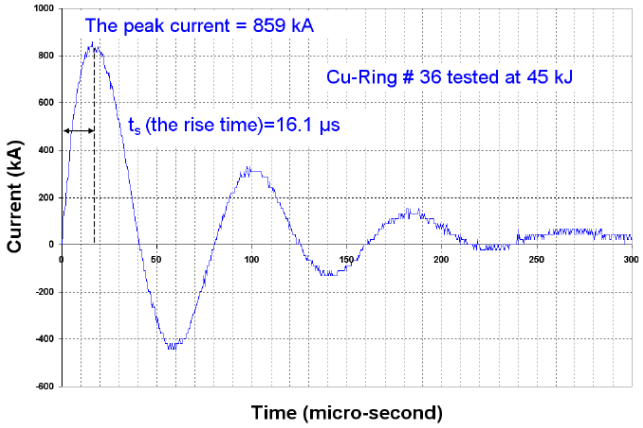

Figure 12. Measured Time-Current Profile for Copper Ring Tested at 45-KJ.

LS-DYNA SIMULATION RESULTS

Figure 13 is the 3D FEM model built by LS-DYNA. It can be seen that this model is actually axisymmetric. To save the computational time, a 2D axisymmetric model was built to simulate the forming of double-flared rings, shown in Figure 14.

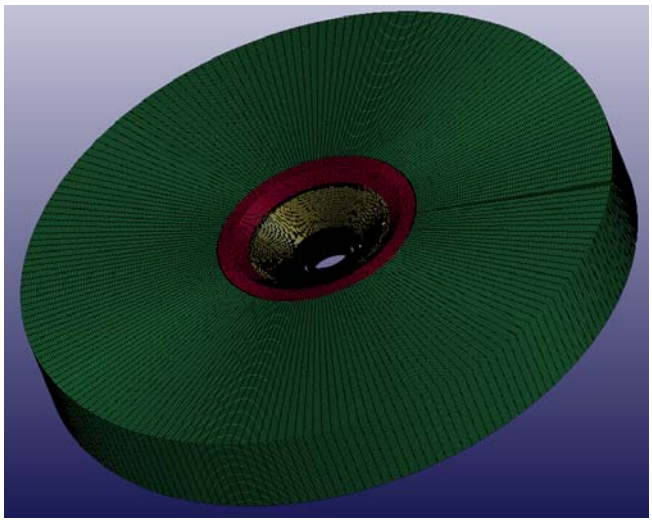

Figure 13. 3D FEM model of double-flared rings with coil and field shapers

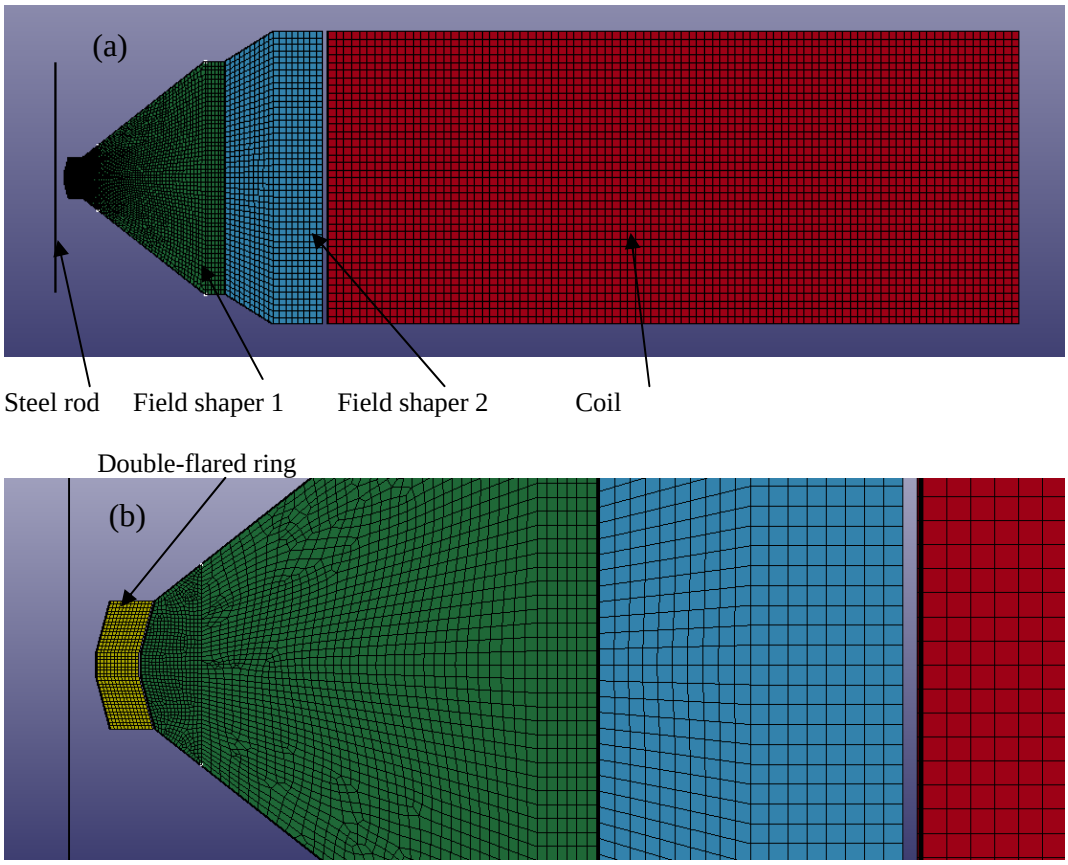

Figure 14. 2D FEM model of double-flared rings with coil and field shapers (a) whole 2D model; (b) closer view

The AISI 4140 steel rod was set as rigid material with shell elements. The double-flared rings of Al 6061-T4 and C18200 were modeled using Johnson-Cook strength model, which is listed in Table 2.

Table 2. Parameters of Johnson-Cook strength model for Al 6061-T6

	A (MPa)	**B (MPa)**	**C**	**n**	**m**	**Tm (K)**
Al 6061-T4 (Johnson, 1983)	110	256	0.015	0.34	1.0	925
Cu (Johnson, 1985)	90	292	0.025	0.31	1.09	1356

Figure 15 shows the simulation results of the 2D simulation for the case of Cu double-flared ring EM formed at 45-KJ. The measured current profile in Figure 12 was set as the input for the simulation. The simulation results indicated that the Cu double-flared ring began to move at 2.80-μs. The middle section of the ring impacted the steel rod at 18.40-μs with the velocity of 282-m/s, shown in Figure 15 (3). The two ends of the Cu ring continued to move forward after the middle section impacted the steel rod. The two ends impacted the steel rod at 19.40-μs with the velocity of 396-m/s. It should be noted that the simulation results indicated that the impact angle was small (around 1~3 degree), shown in Figure 15 (3), (4) and (5). The small impact angle made the impact welding hard to achieve.

The 2D simulation for the case of Al6061-T4 double-flared ring EM formed at 30.6-KJ. The measured current profile in Figure 11 was set as the input for the simulation. The simulation results showed the middle section of Al6061-T4 double-flared ring impacted the steel rod at the velocity of 403-m/s, and the two ends of the Al6061-T4 ring impacted the steel rod at the velocity of 538-m/s. Similar as the Cu double-flared ring, the impact angle was small, around (3~5 degree), which also made the impact welding hard to achieve.

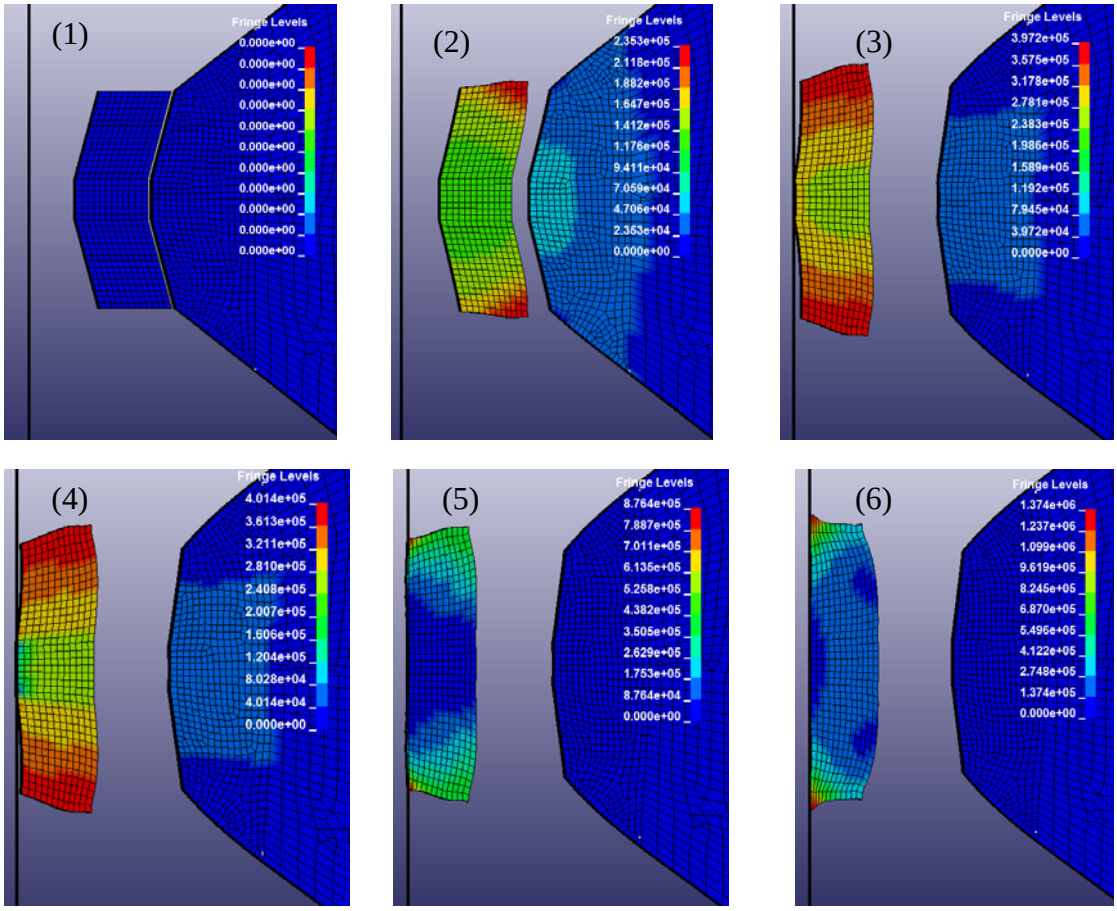

Figure 15. Double-flared Cu ring at different time frame (EM formed at 45-kJ)
(1) t=0-μs; (2) t=10.19-μs; (3) t=18.40-μs; (4) t=19.00-μs; (5) t=20.20-μs; (6) t=21.20-μs

FINDINGS

The following findings can be summarized from this study:

- The single- and double-flared ring samples with a zero gap did not show any reliable joint in test.
- To increase the kinetic energy for welding, the ring-shaft gap was increased to 2-mm and the double-flared ring samples with 2-mm gap showed the improved retentions between the ring and the shaft, but no welding was obtained.
- The double-flared with 2-mm gap showed the best performance in terms of the maximum push-off load.
- Finite-element analysis (FEA) simulation predicted the impact velocity of Cu double-flared ring was at the range of 282-m/s to 396-m/s, and the impact velocity of Al 6061-T4 double-flared ring was at the range of 403-m/s to 538-m/s.
- Finite-element analysis (FEA) simulation predicted the impact angles for both the Cu and Al6061-T4 double-flared ring were small, which made the impact welding hard to achieve.
- The diameter/thickness ratio ~12.0 was found to be difficult to weld for EMW because of small impact angle and thermal damage and melting as the current levels increased.

DISCUSSIONS

In our experiments, the double-flared ring performed better than the single-flare ring. This can be explained by a reason that a single-flared ring caused the unbalanced axial force in the longitudinal direction. This axial force weakens the joint between the ring and shaft, while the normal force on the shaft can increase the joint strength. As a result, a weak joint was obtained in the single-flared ring with the steel shaft as observed in the push-off testing. Aluminum dual-flared ring with zero gap at the higher energy (e.g. #9 sample at 54-kJ) did not give a strong joint with the steel shaft compared to the aluminum dual-flare ring with 2-mm gap at a relatively lower energy (e.g. #24 sample at 24.3-kJ). To obtain the higher impact speed of ring, the gap between the ring and the shaft should be increased. In addition, the amount of discharge energy should be adequately selected to avoid any fracture of aluminum ring after impact. A copper ring did not show any significant fracture in testing, while aluminum rings with 2-mm gap gave fracture at the high discharge energy because of the difference of ductility of two materials. The diameter/thickness ratio is important factor in EMW, particularly when the dimensional constraints of the required assembly design exist. To increase the speed of ring for impact welding, this ratio should be increased by using a thinner ring. However, this can easily results in the fracture of ring. The use of a thicker ring can reduce this fracture issue, however a much larger energy required to accelerate a thicker ring, and the system used in experiments did not have enough capacity to meet these requirements.

CONCLUSIONS

The following conclusions can be drawn from this study:

- No welding was obtained from the EMW tests.
- Mechanical fitting was obtained.
- Aluminum ring samples showed excessive thinning at the edges.
- Maximum push-off loads of ~40-kN were seen for aluminum rings.
- Copper ring samples resulted in push-off loads as high as 80-kN as the best condition of 45-kJ at 2-mm gap.
- Copper rings showed improved shape retention in the as assembled condition compared to aluminum.
- The simulation results showed the small impact angle for both Cu and Al6061-T4 double-flared rings, which made the impact welding hard to achieve.

REFERENCES

Daehn, G. (2005) High Velocity Metal Forming, *ASM Handbook*.

Gourdin, WH (1989) Analysis and assessment of electromagnetic ring expansion as a high-strain rate test, *Journal of Applied Physics*, Vol.65(2), pp.411-422.

Johnson, G. R., and Cook, W. H. (1985) Fracture Characteristics of Three Metals Subjected to Various Strains, Strain Rates, Temperatures and Pressures, Engineering Fracture Mechanics, No. 21, pp. 31– 48

Johnson, G.R., and Cook, W. H. (1983), A constitutive model and data for metals subjected to large strains, high strain rates and high temperatures, Proceedings of the 7th international symposium on Ballistics, pp.541-547, The Hague, the Netherlands

Kim, H., Gould, J., Kimchi, M., Shang, J., Yadav, A., Meyer, R., (2012) Investigation of the Efficiency of Joint Designs for the Electro-Magnetic Welding (EMW) of the Ring-Shaft Assembly, Proceedings of NAMRI/SME, Vol. 40.

Kojima, M, Tamaki, K, and Furuta, T (1989) Effect of Collision Angle on the Result of Electromagnetic Welding of Aluminum", *Transactions of the Japan Welding Society*, Vol. 20, No. 2, pp. 36-42.

Masumoto, I, Tamaki, K, and Kojima, M (1985) Electromagnetic Welding of Aluminum Tube to Aluminum or Dissimilar Metal Cores, *Transactions of the Japan Welding Society*, Vol. 16, No. 2, pp. 14-20.